



Illustrating the active faults using integrated geophysical data along the Suez Canal-district, Eastern Desert, Egypt

Taha Tawfik Rabeh¹ · Ahmed Awad Abd El Rahman¹

Received: 21 November 2021 / Accepted: 20 March 2022 / Published online: 16 April 2022
© The Author(s), under exclusive licence to Springer Nature Switzerland AG 2022

Abstract

Geophysical (magnetic and seismological) data were used to illustrate the subsurface geologically active structures that could be earthquake sources along the Suez Canal-district. The magnetic data required for constructing the magnetic maps was achieved through a land magnetic survey using Gem's Overhauser magnetometer and the Misallat observatory as a base station for data diurnal correction. The magnetic data was then reduced using data from the International Geomagnetic Reference Field. Magnetic analytical techniques were used in a variety of approaches (e.g., reduction to the magnetic pole and the horizontal gradient, 3D analytical signal, 2D and 3D Euler, 3D magnetic modeling, and Curie depth analysis). The findings of the applied magnetics techniques were promising for further magnetic depth estimation models and interpretation of the structural trends. The obtained magnetic anomaly trends follow E–W, NW–SE, and NE–SW directions. The seismological data of the Egyptian National Seismic Networks was processed to show the active faults from the clustering and distribution of earthquake epicenters and to detect their types using the focal mechanism solutions. Eventually, the comparison between the resulted fault structures that prevailed and the earthquake's epicenters shows that the area was identified as having moderate activity for earthquakes in the southern part. The activities of these faults were confirmed by the Curie magnetic depth, which reaches 8 km.

Keywords Land magnetic survey · Seismological data · Curie magnetic depth · Subsurface faults · Suez Canal-district

Introduction

The Egyptian government encourages the establishment of new urban areas that can accommodate both industrial expansion and population growth. So, any new planned area must have a complete view of its subsurface structure. Geophysical surveys provide a tool for viewing the internal structure of the earth and monitoring its environmental impact. Among the geophysical survey tools is the magnetic method, which is the best, most accurate, and easiest of the geophysical survey tools. It has the advantage of imaging the subsurface structures and determining the basement depth due to the differences in the constituent mineral composition of the underlying rocks (Waheed 2019).

The research area is one of the most important portions of the Cairo–Suez sector, which is undergoing an

infrastructural revolution that includes the construction of new cities, ports, and subterranean tunnels. A comprehensive land magnetic survey was conducted in the proposed locations to delineate the subsurface structures and illustrate the active faults that could affect these structures. The inferred fault structures were then correlated with the earthquake epicenters measured by the Egyptian National Seismic Networks (ENSN) with the identification of the fault types.

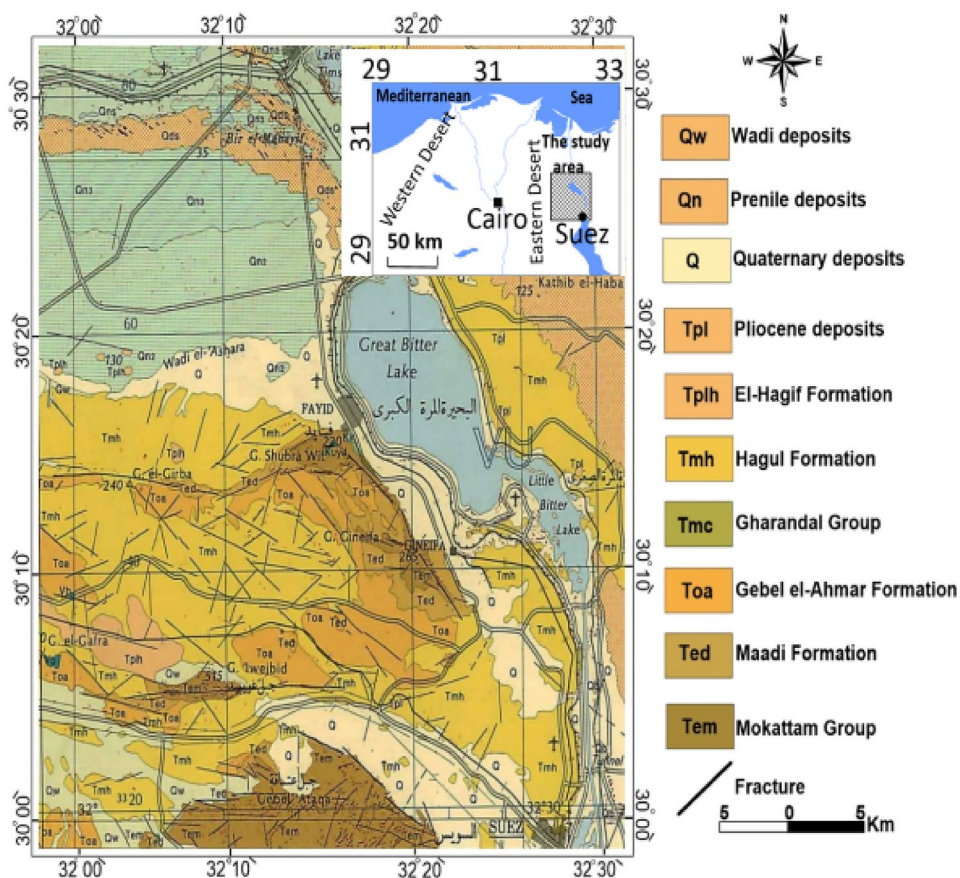
Geological setting

The research area is located in the eastern part of Cairo, between latitudes 29°58' to 30°32' N and longitudes 31°59' to 32°32' E, and covers approximately 3200 km². On looking at the surface geologic map (Fig. 1), it can be noticed that the area is affected by several faults: NW–SE, NE–SW in the middle part, and the faults E–W that are mostly located in the southern part of the study area.

✉ Ahmed Awad Abd El Rahman
ahmedawd4@yahoo.com

¹ Geomagnetism Department, National Research Institute of Astronomy and Geophysics, Helwan, Egypt

Fig. 1 Geological map of Suez Canal-district (modified after Conoco 1987)



There are several earlier geological works that were applied by many scientists that describe the tectonic setting of the area and its surroundings. Abdallah (1964), Strougo (1985a, b), Strougo and Boukhary (1987), Strougo and Abdallah (1990) and Abdallah (1993) concluded that the area has a large number of fault-bounded sedimentary basins which are then filled by abundant and diverse non-marine to deep-marine sedimentary deposits together with the participation of volcanic and volcano-clastic deposits. Bruce and Hotzl (1988), Said (1990), Abou Khadrah et al. (1993), and McClay et al. (1998) stated that the succession of the sedimentary cover in the area ranged from Upper Eocene to Recent age. Through the opening of the Red Sea from the Oligocene until the Middle Miocene period, the Cairo–Suez-district was subjected to active crustal deformation and volcanism that produced deeply buried complex fault and fold structures of the Syrian-Arc System, Zain El-Din et al. (1994) and Hegazi and Omran (1998). The resulted E-W faults during the rifting of the African-Arabian plate were mostly formed in the late Triassic-early Jurassic. These faults were reactivated to affect the tertiary rocks, Hussein and Abd-Allah (2001).

Data and methodology

The data utilized in this study came from the following sources:

A. Land magnetic data

For a period of 3 weeks, Gem's Overhauser magnetometer (GSM-19) was used to conduct a land magnetic survey over the chosen area in the Suez Canal-district. Based on the readings of the magnetic field gradient and field obstacles, the distance between the investigated stations ranged from 100 to 300 m. The position of the measurement stations was detected by the global positioning system instrument (GPS) with 1 m accuracy. At each surveyed location, three to five readings were taken with a 5-min interval between them. Higher scattered magnetic readings of more than 3 nT from their mean values were rejected since they were thought to be a source of magnetic abnormalities, and alternative sites were chosen instead. The Misallat Geomagnetic Observatory was used as a base station for the diurnal correction. This configuration system gives accurate and more detailed

evidence about the subsurface structures and magnetic anomaly disparities.

Finally, the latitudinal correction was applied to the land magnetic data, and the total intensity land magnetic map was obtained (Fig. 2). It revealed that the magnetic field increased in the area with a maximum relief of about 92.4 nT in the southern and northern parts of the area and decreased to a minimum of about -99.3 nT in the northeastern and eastern–western parts of the area. The general magnetic anomalies trend in the NW–SE, NE–SW and E–W directions. The highest magnetic anomalies in southern and western parts of the area were separated from the lowest magnetic anomalies in the northeastern part of the area by a steep gradient, indicating that it is structurally controlled by a major fault trending in the NW–SE direction.

B. Seismological data acquisition

The seismological data for a period of 100 years, including the investigated area and the earthquake data catalogue measured by the Egyptian National Seismological Network center (ENSNC) at the National Research Institute

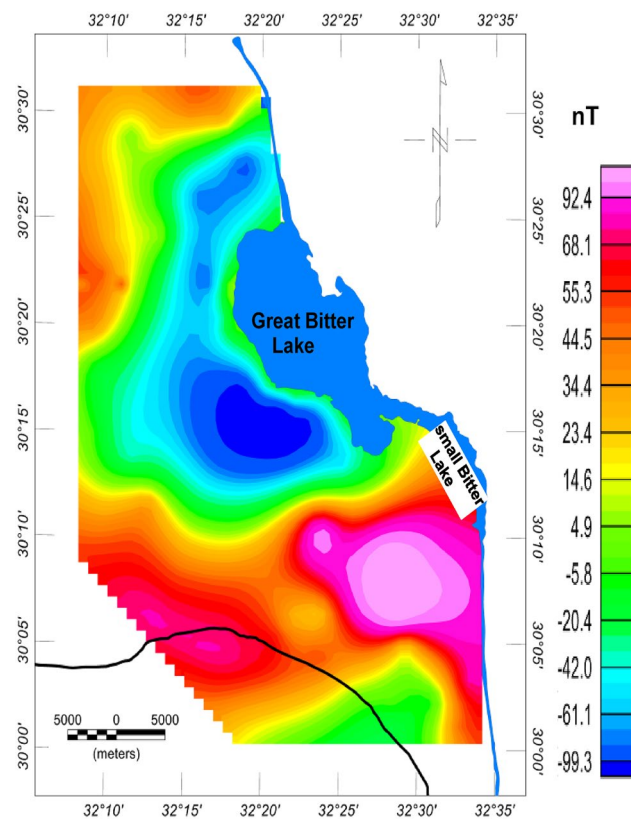


Fig. 2 Total land magnetic intensity map along the Suez Canal-district

of Astronomy and Geophysics (NRIAG), was obtained and subjected to the analyses.

Data enhancement and interpretation

A. Land magnetic data

A.1: Reduction to the north magnetic pole and the horizontal gradient method

Due to the changing declination and inclination angles of the geomagnetic field according to the earth’s coordinates, it causes shifting in the positions of the magnetic field data. So, the reduction to the north magnetic pole technique (RTP) was applied to the total land magnetic data to distinguish the actual setting of the magnetic anomalies that reflect the subsurface structures in the area of study. The total intensity magnetic map was reduced to the northern magnetic using the known inclination and declination of the study area, where the total magnetic intensity is 43200 nT (inclination and declination angle are 44.3 degree and 4.5 degree, respectively). These parameters are used to yield the reduced north magnetic pole and the construction of the RTP magnetic map (Fig. 3). The reduced to the pole map of the study area (Fig. 3) revealed that the magnetic field increases in the area with a maximum relief of about 101.5

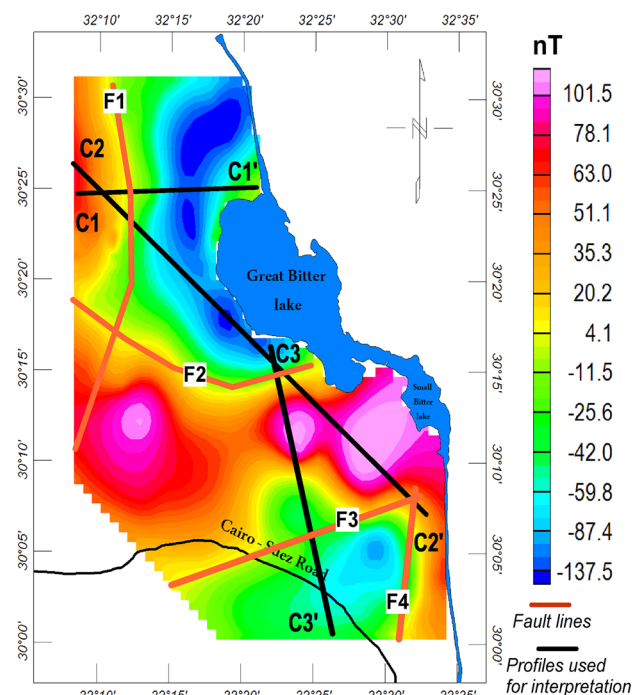


Fig. 3 RTP land magnetic map for the Suez Canal-district showing the interpreted fault structures

nT in the eastern and western part of the area and decreases to a minimum of about -137.5 nT in the northeastern part of the area. The majority of the magnetic anomalies on the RTP land magnetic anomaly map are trending E–W, NW–SE, and NE–SW direction.

The horizontal gradient technique is the simplest filtering method that uses estimates of body contact locations at depths (Roest et al. 1992; Philips 1997). The horizontal gradient approach has a minimal sensitivity to noise in the data because it only involves the calculation of the field's two first-order horizontal derivatives. It has the greatest number of assumptions regarding the sources (Philips 1997). The deduced subsurface fault trends accomplished in this work are based on the Grant and West (1965) approach and Linseer (1967) techniques. The area is affected by four fault structures (F1 to F4), as shown on the map by the brown lines (Fig. 3). It shows high and low magnetic anomalies located in the western and eastern parts of the map. Our concerns are the active fault structures extending from the Gulf of Suez in the east towards the Capital Cairo passing by New Capital, Badr, Madeenty, and El Sherouk cities.

A.2: Depth techniques

Two depth methods were used to determine the depth of the subsurface anomalies: the Euler deconvolution technique and the 3D magnetic modeling technique. The Euler deconvolution technique, published by Reid et al. (1990), enables us to detect the position and depth of magnetic anomaly sources. It displays the contact structure indexes (SI) by integrating both geological and geophysical constraints into a collected and aggregated depth map. The structural index is a measure of the amount of change of the magnetic field with the distance. The technique was applied to the RTP magnetic anomaly map using a 0.5 magnetic step index through the Geosoft program. The resulting data are graphed in (x, y) positions that are proportional to the depth z. The application of the 3D Euler deconvolution techniques confirms the presence of the interpreted structures, whereas the Euler solutions cluster along these structures (Fig. 4).

The second technique to estimate the depth of magnetic anomaly sources is 3D magnetic modeling. The 3D modeling technique relies on the theories of Talwani and Maurice (1960), Grant and West (1965) and Pařteka et al. (2012). The technique was applied to a set of profiles along the RTP magnetic anomaly data using the GM SYS-3D (2006) software. This model permits dealing with the layered structures as isolated bodies, such as igneous intrusions and the stratigraphy of the sedimentary rocks. From the previous information resulting from the drilled wells and determined depth estimation methods, we suggest the basement surface as a

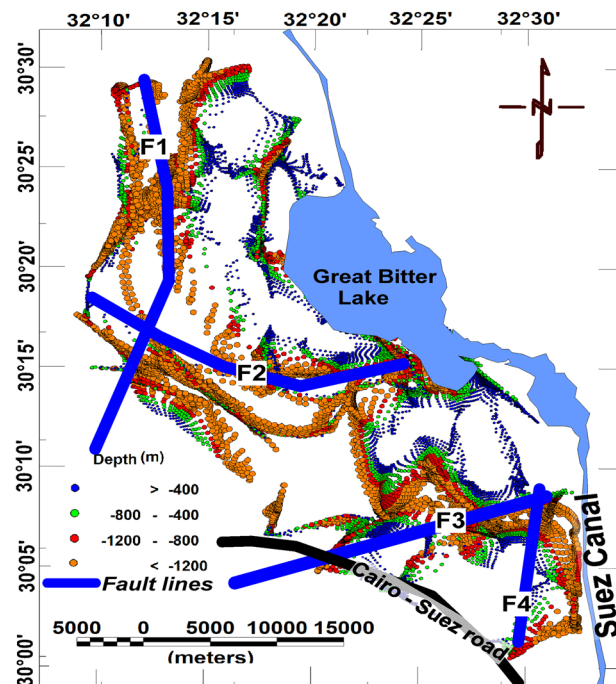


Fig. 4 The 3D Euler deconvolution solutions and the deduced structures from the RTP land magnetic map for the Suez Canal-district

layer. By changing the values of the magnetic susceptibility of the basement rocks and their related intrusions, the fitting between the calculated and the observed magnetic curves is obtained. The sedimentary rock units must change both their magnetic susceptibility and the depth of their boundaries.

The results obtained from the application of the 3D magnetic modeling technique with the horizontal gradient techniques along profiles (C1-C1' and C2- C2') (Figs. 5 and 6) approve the presence of the interpreted fault structures along the RTP land magnetic map. The depth of the basement rocks reaches about 1.3 km.

A.3: Curie magnetic depth method

The term “Curie depth” refers to the depth at which the magnetization of the underlying rocks is close to zero. Based on the Okubo et al. (1985) formula, it is dependent on outlining the distance between the top of magnetic sources and their centers (Z_t and Z_o) using the Fourier transform, which converts the data into frequency domain to acquire the power spectrum, from which we can calculate the depth to the top (Z_b) basement depth and the depth to the centroid (Z_o), then the basal depth (Z_b) will be $(2Z_o - Z_t)$. The resultant Curie depth ranges between 8 km and about 28 km. The shallowest Curie depth is situated at the intersection of the fault structures F3 and F4, along the fault structure F2, and at the NE and NW parts of the investigated area (Fig. 7).

Fig. 5 **a** Horizontal gradient along profile (C1–C1'), **b** 3D magnetic model, and **c** 2D Euler deconvolution with the deduced structures from the RTP land magnetic map for the Suez Canal-district

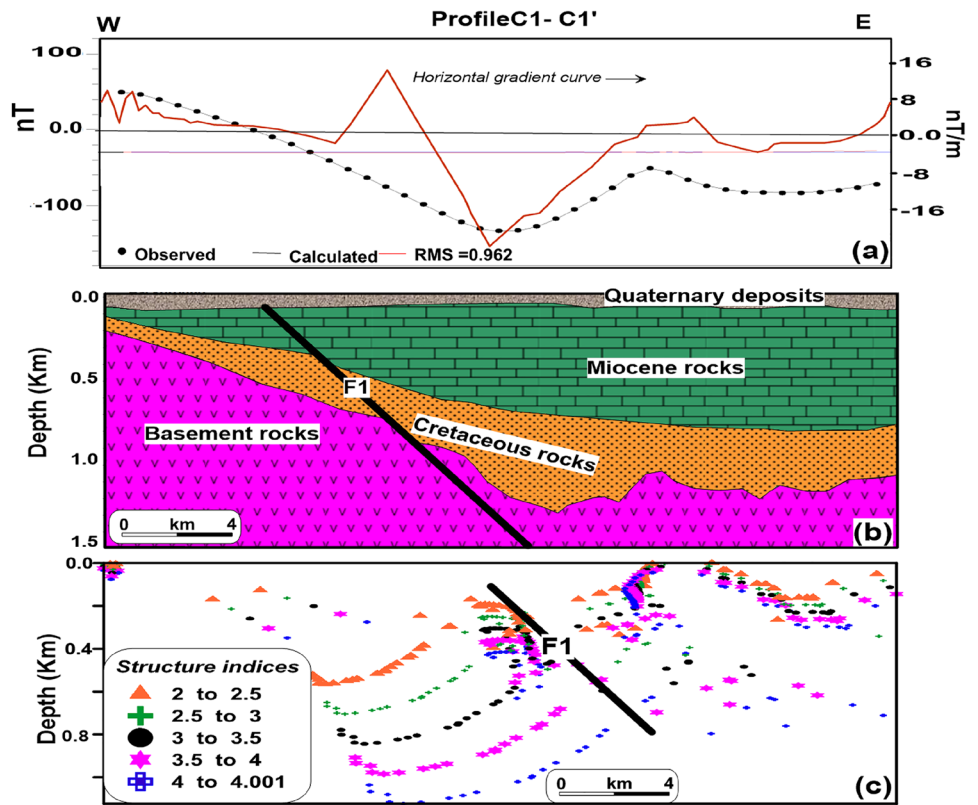
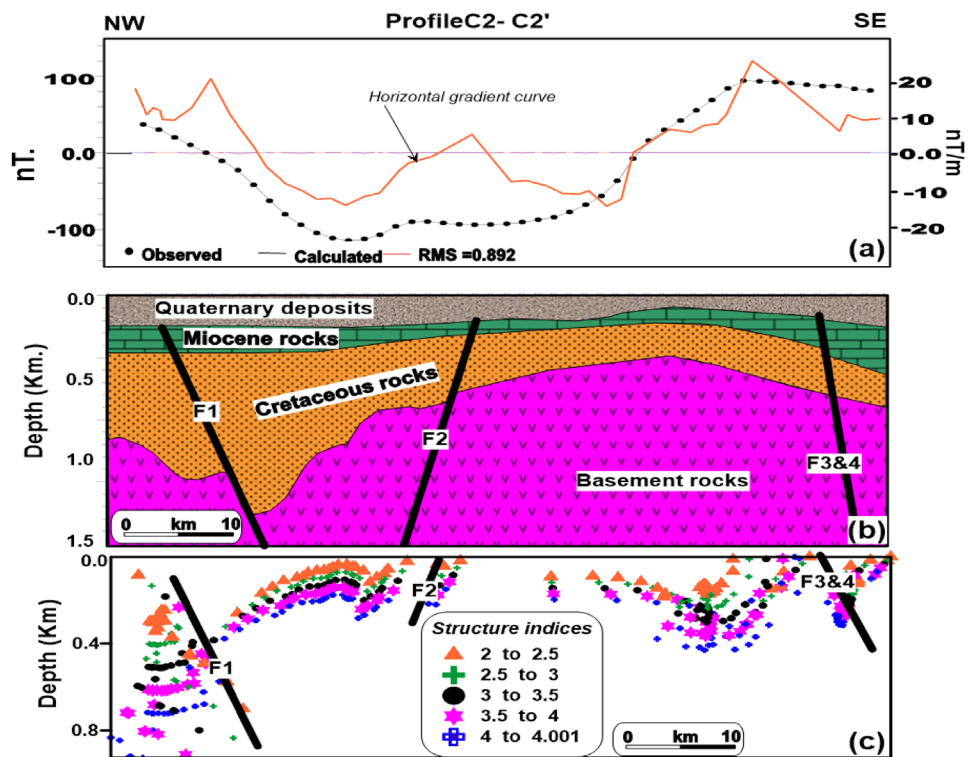


Fig. 6 **a** Horizontal gradient along profile (C2–C2'), **b** 3D magnetic model, and **c** 2D Euler deconvolution with the deduced structures from the RTP land magnetic map for the Suez Canal-district



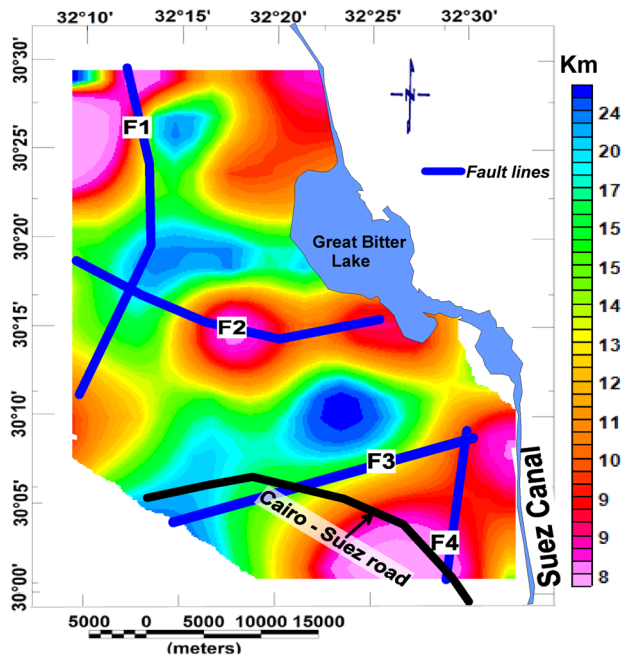


Fig. 7 Curie magnetic depth and the deduced fault structures interpreted from the RTP land magnetic map for the Suez Canal-district

B. Seismological data

B.1: Correlation between fault structures and earthquake's epicenters

The seismological data of the ENSN was processed to show the active faults from the distribution of earthquake epicenters and to detect their types using the focal mechanism solutions. The focal mechanism and seismological approaches are critical for understanding the different types of the seismic faults, as it reveals information about the plate motions, the tectonics around the earthquake source region, and the tectonic stresses that cause earthquakes. The analysis of seismic waves is based on the seismic fault model of earthquakes. The model used in this study was performed by (Abu El Enean 1997), who used the solutions from the Global Centroid Moment Tensor database (formerly known as the Harvard CMT catalogue) to study regional tectonic stresses. The focal mechanism solution was applied to the seismological data in the investigated area to confirm the existence of the fault structures inferred from the land magnetic data. Two earthquake focal mechanisms analyses were used to analyze the data (Fig. 8). The most active seismicity regions are sited near to the intersection of the fault structures F3 and F4. In addition, the fault structure F2 shows some moderate seismicity, whereas F1 shows low seismicity for earthquakes of 2 magnitudes.

The correlation between the interpreted fault structures and the earthquake's epicenter distributions for earthquakes

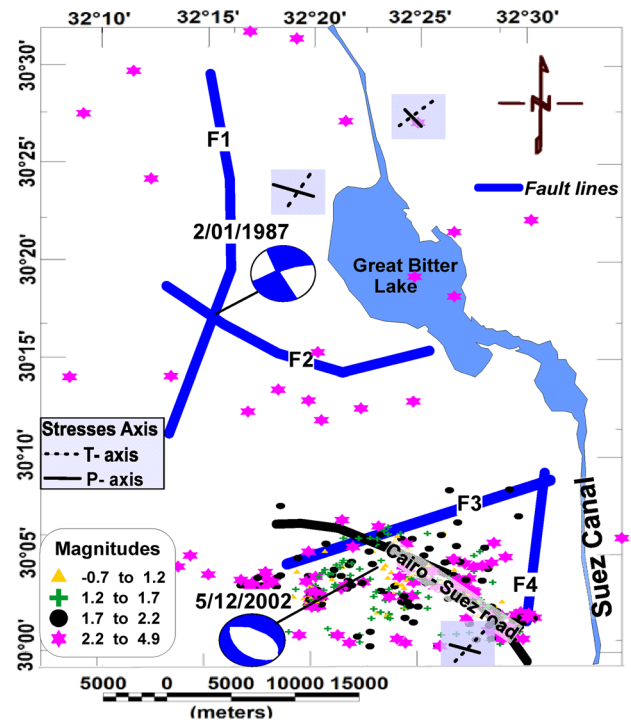


Fig. 8 Focal mechanism solutions for earthquakes in the Suez Canal-district. Also, it shows the distribution of the earthquake's epicenters along with the fault structures derived from the interpretations of RTP land magnetic map

recorded by ENSN from years 1987 to 2017 shows that the most active zones are located near the detected fault structures, especially the Cairo-Suez fault structure. The two calculated focal mechanism solutions show that the type of these faults is normal faults (Fig. 8). The stress fields of the measured seismic zones were selected based on the deduced focal mechanism, and the average direction of the tension axis (*T*-axis) and pressure axis (*P*-axis) was calculated. The *T* and *P* axes' spread across the area (Fig. 8), shows a main *T*-axis trending around N 45° E. The surface faults illustrate that there are extensional stresses active in the southern part of the area along the normal fault F4, while the focal mechanism solution of 2/01/1987 in the northern part of the investigated area shows a strike-slip fault.

Conclusions

The integration of the geophysical techniques, including the magnetic and seismic data, was applied at the Suez Canal-district to illustrate the main active faults that may be responsible for earthquakes. The data resulting from the magnetic survey was analyzed and interpreted to give an indication of the tectonics that prevailed in the study area. The correlation between the deduced fault structures and

the allocation of the epicenters of the earthquakes recorded by (ENSNC), revealed the activities of these detected fault structures. Their types were then recognized from the focal analysis solutions of the seismological data. The comparison between the resulted fault structures that prevailed in the investigated area and the earthquake's epicenters shows that the proposed area is identified as having moderate activity for earthquakes in the southern part of the investigated area. The locations and geometry of these structures and the depths to the basement rock surface were obtained using horizontal gradient, 2D and 3D modelling techniques for the magnetic data, where the obtained depth ranges from 200 to 1300 m to the basement rocks. In addition, the 3D Euler deconvolution techniques of 0.5 magnetic indexes confirm the existence of the deduced structures. The Curie magnetic depth estimated along the study area reaches less than 12 km, reflecting the moderate activity of these fault structures. Finally, we can conclude that the earthquake impact factor should be taken into consideration for urban and infrastructure development, particularly in the southern part of the investigated area.

Acknowledgements The current work was carried out as part of Project No. 5518, which was funded by Egypt's Science and Technology Development Fund (STDF).

Declarations

Conflict of interest The authors declare that they have no conflict of interest with respect to the research, authorship, and publishing of this article.

References

- Abdallah AM (1964) New Bathonian (Middle Jurassic) occurrence at the western side of the Gulf of Suez. Egypt. In: Geological Survey, Paper No. 30, pp 1–8
- Abdallah AMA (1993) Structural geology of the area between El-Galala El Bahariya and Gebel Okheider. Ph.D. thesis, Faculty of Science, Ain Shams University, Cairo, pp 1–199
- Abou Khadrah AM, Wali AMA, Müller AMA, El Shazly AM (1993) Facies development and sedimentary structures of syn-rift sediments, Cairo-Suez District. Egypt Bull Fac Sci Zagazig Univ 15(2):355–373
- Abu El Enean KM (1997) A study on the seismotectonic of Egypt in relation to the Mediterranean and Red Seas tectonics. Ph.D. thesis, Faculty of Science, Ain Shams University, Cairo, pp 1–200
- Bruce H, Hotzl H (1988) The sedimentary evolution of the Red Sea rift: a comparison of the northwest (Egyptian) and northeast (Saudi Arabia) margins. Tectonophysics 153:193–208
- Conoco (1987) Geologic map of Egypt. In: Egyptian General Authority for Petroleum (UNESCO Joint Map Project), 20 Sheets, Scale 1:500 000, Cairo
- Grant FS, West GE (1965) Interpretation theory in applied geophysics. In: Geological magazine, vol 103(2). McGraw-Hill, New York, p 184
- Hegazi AM, Omran MA (1998) Structural analysis of Shabrawet area, Northeastern Desert, Egypt. Int Conf Geol Arab World (GAW4) Cairo Univ 1:91–106
- Hussein IM, Abdallah AMA (2001) Tectonic evolution of the north-eastern part of the African continental margin. Egypt J Afr Earth Sci 33:49–68
- Linseer (1967) Investigation of tectonics by gravity detailing. Geophys Prospect 15(3):480–515
- McClay K, Nichols GJ, Khalil SM, Darwish M, Bosworth W (1998) Extensional tectonics and sedimentation, eastern Gulf of Suez, Egypt. In: Purser BH, Bosence DWJ (eds) Sedimentation and tectonics in Rift Basins, Red Sea-Gulf of Aden. Chapman and Hall, London, pp 223–238
- Okubo Y, Graf RJ, Hansen RO, Ogawa K, Tsu H (1985) Curie point depths of the island of Kyushu and surrounding area, Japan. Geophysics 50(3):481–489
- Philips JD (1997) Potential field geophysical software for the PC version 2.2. In: USGS open file report 97-725
- Pästeka R, Karcol R, KusnirakMojzes DA (2012) REGCONT, a Matlab based program for stable downward continuation of geophysical potential fields using Tikhonov regularization. Comput Geosci 49:278–289
- Reid AB, Allsop JM, Granser H, Millett AJ, Somerton IW (1990) Magnetic interpretation in three dimensions using Euler deconvolution. Geophysics 55:80–91
- Roest WR, Verhoef J, Pilkington M (1992) Magnetic interpretation using the 3-D analytical signal. Geophysics 57:116–125
- Said R (1990) Cenozoic. In: Said R (ed) Geology of Egypt. Balkema, Rotterdam, pp 451–486
- Strougo A (1985a) Eocene stratigraphy of the eastern Greater Cairo (Gebel Mokattam-Helwan) area. Middle East Research Center in Shams University. Sci Res Ser 5:1–39
- Strougo A (1985b) Eocene stratigraphy of the Giza Pyramids plateau. Cairo: Ain Shams University. Middle East Research Center. Sci Res Ser 5:79–99
- Strougo A, Abdallah (1990) Mokattam stratigraphy of north Eastern Desert (South of Maadi Qattamyia road). M.E.R.C. Ain Shams Univ Earth Sci Res Ser 4:152–175
- Strougo A, Boukhary MA (1987) The Middle Eocene-Upper Eocene boundary in Egypt. Rev Micropaleontology 30(2):122–127
- Talwani M, Maurice E (1960) Rapid computation of gravitational attraction of three-dimensional bodies of arbitrary shape. Geophysics 25(1):203–225
- Waheed HM (2019) Geophysical studies for hydrocarbon reservoir exploration at west Beni Suef Area. Al-Azhar University, Faculty of Science, Geology Department, M.Sc., Western Desert
- Zain El-Din MY, Darwish M, Bakry G (1994) Basin development and hydrocarbon potentials of the south Nile Delta provinces, Egypt. In: 2nd international conference on Geological Arab World, Cairo University, Egypt, pp 185–218

Publisher's Note Springer Nature remains neutral with regard to jurisdictional claims in published maps and institutional affiliations.